

A Cost-effective Production Method for High-precision MM-wave Waveguide Antennas and Components

Invited Paper

Alexander Vorobyov
CSEM: Centre Suisse d'Electronique et
de Microtechnique SA, Neuchatel,
Switzerland,
oleksandr.vorobyov@csem.ch

Samuel Unterhofer
CSEM: Centre Suisse d'Electronique et
de Microtechnique SA, Neuchatel,
Switzerland,
samuel.unterhofer@csem.ch

Olha Sereda
CSEM: Centre Suisse d'Electronique et
de Microtechnique SA, Neuchatel,
Switzerland,
olha.sereda@csem.ch

Abstract—This paper presents a cost-effective production method for high-precision, complex 3D mm-wave components and antenna prototyping. The selected manufacturing process, Laser Powder bed fusion, has been optimized for high printing resolutions. Two mm-wave (75-110GHz) structures have been designed, prototyped and characterized. These are hollow waveguide sections and iris-based phase shifters.

Keywords—mm-wave antenna, waveguide, additive manufacturing, 3D printing

I. INTRODUCTION

Traditional manufacturing of waveguide mm-wave antennas usually includes manual assembly steps and the success of a functional antenna is largely owing to good craftsmanship. The diffusion-bonding and split-block solutions are most technologically advanced than conventional methods. As a result, they are very expensive and time-consuming to prototype. It is estimated that around 70% of final assemblies do not meet the performance requirements after testing and must be scrapped. Additive manufacturing brings 2 advantages that can overcome the production process: a repeatable quality thanks to the single manufacturing operation (strongly reduced assembly and conservation of critical parameters) and fewer assembly steps.

A comparison table of different manufacturing methods is presented in Table 1.

TABLE I. MANUFACTURING METHODS

Property	Diffusion bonding	Split-block	L-PBF
Process complexity	+	-	+
Parts complexity	+	++	++
Different metals	+	+	++
Accuracy	++	++	+
Mass production	+	-	++
Production cost	+	-	++
Legend	-hard or difficult	+ good with small limitations	++ highly possible

A cost-effective production method for high-precision mm-wave waveguide antennas with 3D printing has been discussed in [1]-[10].

The paper presents an efficient and affordable production method for high-precision mm-wave waveguide antennas. The selected manufacturing process, Laser Powder bed fusion (L-PBF), is a metal Additive Manufacturing (AM) technology that has been optimized for high printing resolutions at CSEM. Building parts layer by layer, by depositing material according to the digital 3D design data. This process allows for the fabrication of parts that are difficult or impossible to be produced with traditional machinings, such as high-precision mm-wave components.

The 3D printed parts were benchmarked against traditional manufacturing processes (i.e. machined). L-PBF vs traditional manufacturing comparison.

TABLE II. L-PBF VS MACHINING

Criteria	Project Goals	SoA machining
Manufacturing technology	L-PBF	Rotary cutting tools
Manufacturing tolerance	<10 μm	10-50 μm
Surface roughness	<1 μm	>1 μm
Production cost (identical product)	Reduction of costs by 20% - 50%	Depends on complexity
Attenuation loss (scrap rate)	4-6dB/m	3-5dB/m (commercial solutions)
Mass reduction	>10%-15%	Depends on the process
Waste reduction	>20%-40%	Depends on the process

This paper is organized as follows: Section II describes the prototyping aspects. Section III describes the realized hollow waveguide section and compares its performance with the micromachined one. The realised WG-based phase shifters are discussed in Section IV. The conclusion is provided in Section V.

II. PROTOTYPING ASPECTS

The full chain process optimization (Fig. 1) consists of three complementary parts: Feedstock materials, the LPBF process and post-processing. Aluminium-silicon alloy has been the selected material to prototype mm-wave RF components, based on its elevated surface roughness quality, electrical and mechanical properties, and cost.

The electrical conductivity of the selected material is between 4e-8 Ohm·m and 6e-8 Ohm·m after one hour of the thermal post-treatment for 400°C and 200°C accordingly.

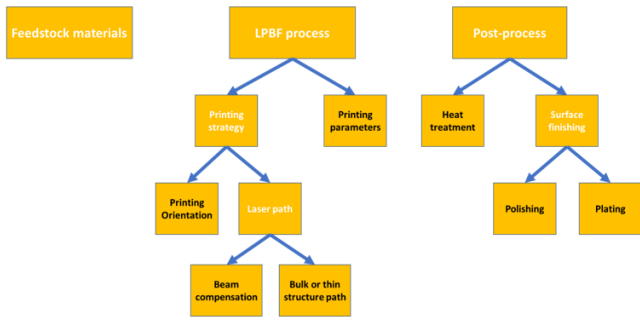


Fig. 1: Full chain 3D printing process

For any component printed, an adaptation of the printing orientation, the laser path and the chemical polishing needed to be developed, since these last are depending on the design.

On the other hand, printing parameters (for bulk structure), heat treatment and electroless silver plating are just slightly dependent on the design; the condition used to perform these last three processes are the same for the 3D printed mm-wave components and antennas.

A. Heat treatment.

Fig.2 presents the impact of heat treatment on the improvement of RF in printed Al12Si. Heat treatment of printed samples leads to improvement of electrical conductivity which improves WG efficiency.

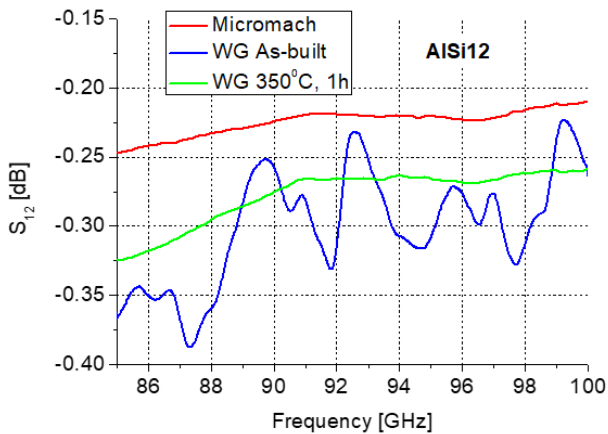


Fig. 2: Influence of heat treatment of printed Al12Si on RF performances

B. Chemical polishing.

The performance of a waveguide depends directly on internal channel roughness and the size of the channel. Chemical polishing is one of the few techniques that can be used to decrease the surface roughness of internal structures, due to its penetration depth capability, but like with any technique, it has disadvantages, such as maintaining the shape and dimensional accuracy of edges and walls. This aspect should be considered during the RF component design.

C. Printing strategy.

Printing orientation, as a part of the printing strategy, is an extremely important factor that can be used to achieve small as-built roughness on all the inner surfaces. Different RF element orientations are presented in Fig. 3. The most preferable printing orientation depends on the RF component complexity and design.

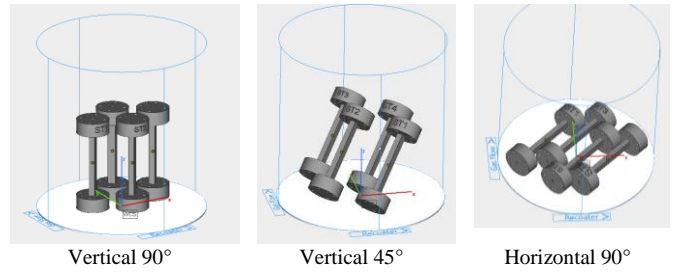


Fig. 3: Printing orientations examples

Table 3 shows the roughness achieved at CSEM with aluminium-silicon alloy, as a function of the surface as-built orientation related to the built direction.

TABLE III. ARITHMETIC SURFACE ROUGHNESS AT DIFFERENT PRINTING ORIENTATIONS

	Up-Skin			Down-Skin			
	90°	60°	45°	0°	60°	45°	0°
Sa	6.3μm	8.0μm	10.1μm	11.6μm	8.4μm	9.6μm	28.1μm

D. Electroless silver plating

To improve the surface conductivity which directly impacts the RF performances, the samples were coated with a thin silver layer using electroless deposition.

In the case of the as-built printed Al-12-Si sample, the deposited coated thickness was measured, using a Focused Ion Beam cross-section, to be about 11μm. The roughness of the surface is about 7 μm Ra before and after treatment, showing that silver plating does not affect the surface roughness.

III. HOLLOW WAVEGUIDE

Many 3D-printed WR-10 WG sections have been prototyped and characterised (Fig.4).



Fig. 4: 3D printed hollow WR-10 WG sections.

A printed and post-processed Al-12-Si sample performance is compared with the standard high-quality micromachined section (Fig.5). Both sections are WR-10 50mm long waveguides.

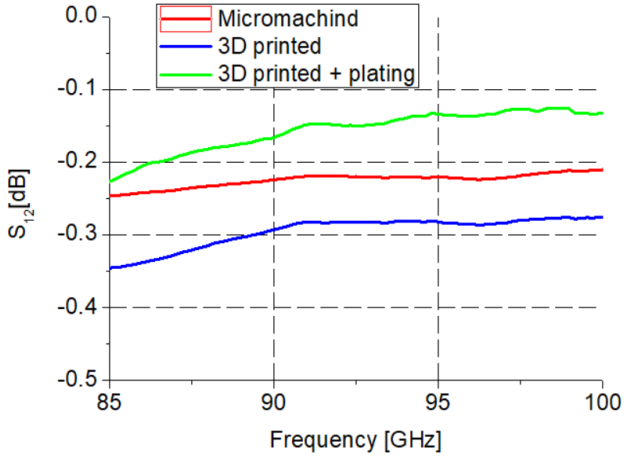


Fig. 5: Comparison of the 3D printed and micromachined 50mm long WG sections.

The measurement result shows that the 3D printed and post-treated WG section performs similarly or better than the micromachined one. Overall 3D printed WG losses lie between 4-6 dB/m. The deviation between the performance of the prototyped waveguides is minimal and is mainly due to the mechanical machining quality of the WG flanges. The quality of the flange surface and the WG aperture drastically influence the loss level.

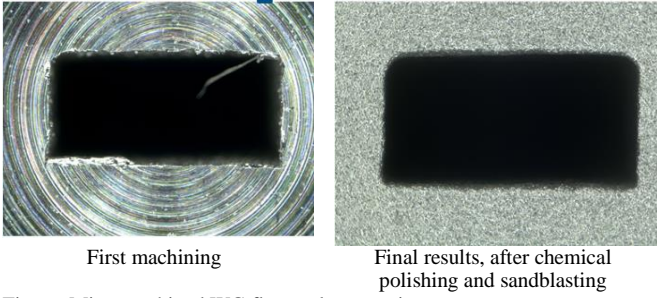


Fig. 6: Micromachined WG flange close-up view.

IV. PHASE SHIFTER

To check L-PBF 3D-printing limitation, a more complex WG-based phase shifter RF component structure has been suggested.

The proposed phase shifter is based on a 3-pole inductive bandpass filter operating at 94 GHz. The phase shifter is integrated into the WR-10 waveguide (1.27×2.54mm²), which is suitable for the 75GHz-110GHz frequency band (Fig.7).

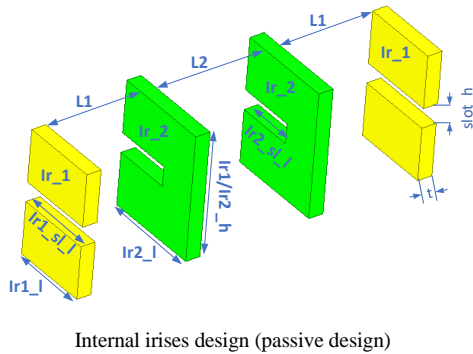


Fig. 7: Phase shifter model

This filter configuration provides good performances in terms of filtering property, S-parameters, manufacturing

complexity, and above all, broad bandwidth. Inductive irises are often used as coupling elements in rectangular waveguide bandpass filters (BPF).

We only consider passive designs as illustrated in Fig 7. Each of the four irises is 3D printed directly in the waveguide. The irises are loaded by a central slot whose length sl_1 and configuration are presented in Table 3.

The filter properties can be tuned by changing the configuration of each slot. This can be done by modifying the length of the slot.

Four passive phase shifters have been designed to provide four different transmission phase responses (Fig.8) with a nearly 2-bit resolution (i.e. with a 90° shift between each phase response at 94GHz).

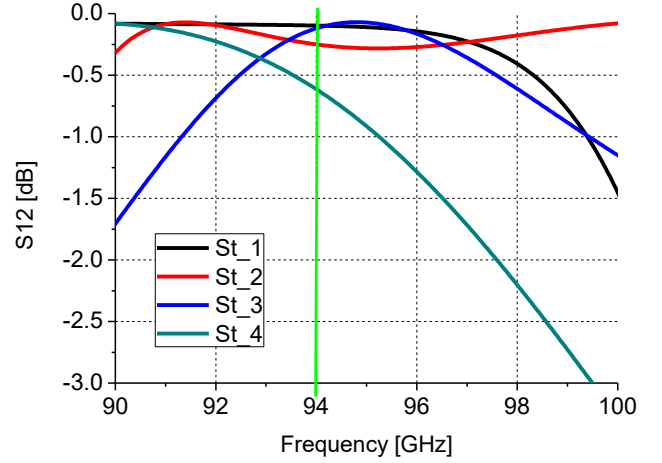


Fig. 8: Theoretical phase shifter S12-parameter.

The dimensions of each iris for the four-phase states are provided in Table 4. The theoretical equivalent bit resolution is equal to 1.9bit.

TABLE IV. FOUR PHASE SHIFTERS DIMENSIONS AND THEORETICAL PHASE VALUE ESTIMATION.

Value [mm]	State_1	State_2	State_3	State_4
L1	1			
L2	1.15			
t	0.2			
h	1.27			
slot_h	0.2			
Ir1_l	0.8			
Ir2_l	1			
N_bit	1.96			
Phase [deg]	-159	90	13	-71
Ir1_sl_1	0.8	0	0	0.8
Ir2_sl_1	0.8	0	0.6	0.6

Four WG sections with the phase shifter elements were prototyped. The best laser path and part printing orientation in relation to the horizontal built plate was applied. The horizontal 90° orientation gives the best quality for the structures inside the channel, but as a compromise, one surface will have a 0° downskin surface, meaning low quality. To resolve this problem, the samples can be post-process by EDM (electrical discharge machining).

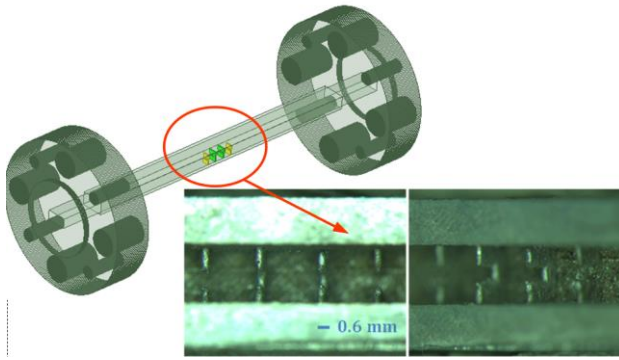


Fig. 9: Phase shifter structures after polishing

The transmission coefficients of the four prototyped phase shifters are represented in Fig.8. The equivalent bit resolution is equal to 1.93bit. However, the losses are much higher in comparison with theoretical estimation.

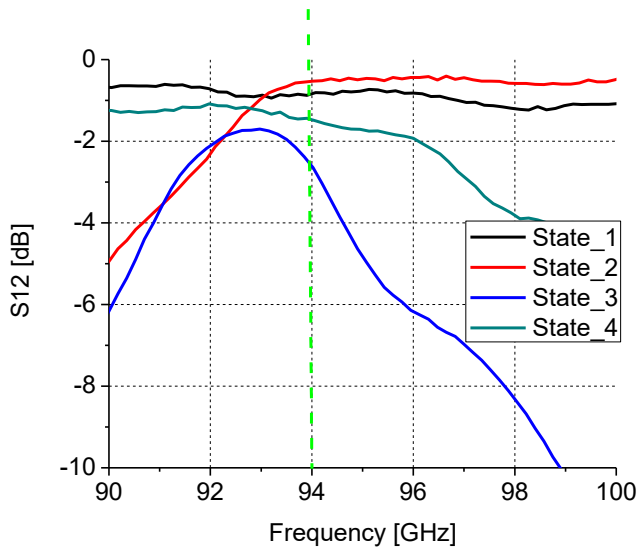


Fig. 10: Measured phase shifter S12-parameter.

TABLE V. PHASE SHIFTER PARAMETER COMPARISON TABLE

State	State_1		State_2		State_3		State_4	
	Teor	Meas	Teor	Meas	Teor	Meas	Teor	Meas
S12 [dB]	-0.1	-0.55	-0.26	-0.89	-0.11	-2.5	-0.62	-1.48
Phase [deg.]	150	126	1.7	33	-72	-61	-159	-124

V. CONCLUSION

The design freedom provided by L-PBF technology has already shown many advantages in micro-wave components manufacturing, such as weight reduction, assembly simplification and cooling channel integration. 3D printing is a good technology choice to produce antennas with complex 3D shapes (e.g. waveguide), assembly steps reduction and costs.

The 3D printed waveguide demonstrated similar and better performance as well as good repeatability in comparison with a standard micromachined solution.

3D-printed waveguide-based phase shifters have been prototyped and characterised. Measurement results show higher losses in comparison with the theoretical estimation. This is due to the prototyping limitation. The ways to overtake the prototyping and postprocessing limitation are under investigation.

ACKNOWLEDGEMENT

The research leading to these results has received funding from the Clean Sky Programme under grant agreement no. 886696 and was carried out in the frame of the 3DGUIDE project (Feasibility demonstration of 3D printing for a new efficient production method of mm-wave waveguide antenna).

REFERENCES

- [1] Yeonsu Lee, "Two-way Waveguide Power Divider using 3D Printing and Electroless Plating, 2018 EuMC.
- [2] M. D'Auria, W. J. Otter, J. Hazell, B. T. W. Gillatt, C. Long-Collins, N. M. Ridler and a. S. Lucyszyn, "3-D Printed Metal-Pipe RectangularWaveguides," *IEEE Transactions on Components, Packaging and Manufacturing Technology*, Vols. vol. 5, no. 9, p. pp. 1339–1349, Sept 2015.
- [3] E. Decrossas, T. Reck, C. Lee, C. Jung-Kubiak, I. Mehdi and G. Chattopadhyay, "Evaluation of 3D printing technology for corrugated horn antenna manufacturing," in *IEEE International Symposium on Electromagnetic Compatibility (EMC)*, 2016.
- [4] J. Shen, M. W. Aiken, M. Abbasi and D. P. Parekh, "Rapid Prototyping of Low Loss 3D Printed Waveguides for Millimeter-Wave Applications," in *IEEE MTT-S International Microwave Symposium (IMS)*, 2017.
- [5] S. Unterhofer, O. Sereda, O. Vorobyov, M. Dadras, "Additive manufacturing of smart waveguide: comparison between three alloys, Bronze, Al-Si andScalmalloy", European Congress and Exhibition on Advanced Materials and Processes 2021
- [6] Otter, William J., and Stepan Lucyszyn. "Hybrid 3-D-printing technology for tunable THz applications." *Proceedings of the IEEE* 105.4 (2016): 756-767.
- [7] Kunchen Zhao, "3D-Printed Frequency Scanning Slotted Waveguide Array with Wide Band Power Divider", USNC-URSI-NRSM, 2019
- [8] Saranraj Karuppuswami,"Effect of Surface Roughness on Material Characterization using 3D Printed Waveguides at W-Band", *AMTA, 2021*
- [9] Xiaobang Shang, "A compact Ka-band waveguide orthomode transducer fabricated by 3-D printing", EuMC, 2016
- [10] Jiayu Rao, "3D Metal Printed Corrugated Waveguide Antenna Array With High Gain and Enhanced Bandwidth", ICSJ, 2021